Benefit of inserting a (Cu/Pt) intermixing dual barrier for the blocking temperature distribution of exchange biased Co/(Cu/Pt)/IrMn stacks

K. Akmaldinov, S. Auffret, I. Joumard, B. Dieny, V. Baltz

APPLIED PHYSICS LETTERS **103**, 042415 (2013)

Benefit of inserting a (Cu/Pt) intermixing dual barrier for the blocking temperature distribution of exchange biased Co/(Cu/Pt)/IrMn stacks

K. Akmaldinov,[1,2] S. Auffret,[1] I. Joumard,[1] B. Dieny,[1] and V. Baltz[1,a)]
[1]*SPINTEC, UMR 8191 CNRS/INAC-CEA/UJF-Grenoble 1/Grenoble-INP, F-38054 Cedex, France*
[2]*CROCUS Technology, F-38025 Grenoble, France*

(Received 11 June 2013; accepted 12 July 2013; published online 25 July 2013)

Exchange bias based spintronics devices involve ferromagnetic/antiferromagnetic interfaces and concomitant layers intermixing. As a consequence, interfacial spin-glass-like phases with reduced properties and increased dispersions form and lower the device performance. It is therefore necessary to limit intermixing by introduction of diffusion barriers. One of the major difficulties is that the barrier must be inert. This paper uses blocking temperature distributions to quantify the interfacial quality of Co/IrMn based stacks. Inserting a (Cu/Pt) dual barrier fulfils the manifold requirements of limiting Co-Mn, Co-Pt, and Cu-Mn intermixing, which takes place when using either no or single Pt and Cu barriers, respectively. © *2013 AIP Publishing LLC*. [http://dx.doi.org/10.1063/1.4816816]

Spintronics applications[1] use ferromagnetic (F)/antiferromagnetic (AF) exchange bias (EB) interactions[2,3] to set the reference direction required for the spin of conduction electrons. They therefore may involve layers intermixing originating from F/AF interfaces.[4–7] As a consequence of intermixing, interfacial spin-glass-like phases with reduced EB properties and increased dispersions form and may lower the devices performances.[8–17] It is thereby necessary to limit intermixing. Diffusion barriers have been commonly implemented in the field of electronics.[18–20] Although the science of diffusion barriers involves many aspects which often lead to compromise,[18] one of the major difficulties is that the barrier must not corrupt the surrounding materials that it is supposed to be protecting. Some barriers may consist of multiple layers to accommodate such a need for non-reactivity.[19,20] Here, we implement diffusion barrier and, in particular, dual barriers for the F/AF building block of spintronics devices. In particular, we focus on F/AF cobalt/iridium-manganese (Co/IrMn) based stacks. This paper uses blocking temperature distributions (DT_B)[12,21] to quantify the interfacial quality of the F/AF interface, where T_B is the temperature (T) over which the AF is no longer thermally stable when cycling the F magnetization.[2,3] In fact, it is now accepted that EB is ascribed to the ability of both AF grains (domains) and AF interfacial spin-glass-like phases to withstand F magnetization reversal.[8–17,21,22] The specific procedure commonly carried out for measurements of DT_B above 300 K (Ref. 21) combined with the alternative use of a sufficiently low reference-T recently provided a method for probing the low-T contribution to DT_B related to interfacial spin-glass.[12] We expect that inserting a copper/platinum (Cu/Pt) dual barrier between Co and IrMn will fulfil the manifold requirements of limiting the various species intermixing which takes place when using either no or single barriers[4–7,11,17,23–25] and that this will translate into less glassy interfaces, i.e., into the observation of lower T_B dispersions.

In this study, Ta (3 nm)/Cu (3 nm)/Co (3 nm)/Cu (t_{Cu})/Pt (t_{Pt})/IrMn (7 nm)/Pt (2 nm) and Ta (3 nm)/Cu (3 nm)/IrMn (7 nm)/Pt (t_{Pt})/Cu (t_{Cu})/Co (3 nm)/Pt (2 nm) are deposited at room-T by magnetron sputtering onto thermally oxidised silicon substrates, Si/SiO_2.[12] The Ta (3 nm)/Cu (3 nm) bilayer is used as buffer, and the Pt (2 nm) film is the capping layer. Co (3 nm) is the ferromagnet, and IrMn (7 nm) is the antiferromagnet made from an $Ir_{20}Mn_{80}$ target. The Cu and Pt thicknesses of the (Cu/Pt) and (Pt/Cu) intermixing dual barriers are t_{Cu} and t_{Pt}, respectively, and take values between 0 and 6 nm. Thick barriers are used here in order to study complete films. Room-T EB is set by post-deposition field cooling (FC) of the samples for 1 h in a furnace from 573 K down to room-T. The positive magnetic field during cooling is applied in the samples planes, and its amplitude of 2.5 kOe is large enough to saturate the Co layers. Following this initial FC, all the AF entities with T_B larger than room-T are oriented toward the positive direction.[12] Room-T hysteresis loops are then measured. Subsequent initial positive FC is continued from 400 to 4 K in the variable T insert of a vibrating sample magnetometer (VSM). DT_B in the range of 4–400 K are then deduced from hysteresis loops measured at 4 K with the VSM after a specific procedure which includes FC from incremental annealing temperatures (T_a). The procedure and typical hysteresis loops are thoroughly detailed elsewhere.[12,21] In brief, after initial positive FC from 573 to 4 K, all the AF entities contributing to EB orient positively. The resulting hysteresis loop shift (H_E) is negative and maximum in amplitude (see $T_a = 4$ K in Fig. 1). From this initial state the AF entities are progressively reoriented by use of negative FC down to 4 K from incremental T_a. The AF entities with T_B lower than T_a reverse. A hysteresis loop is measured at 4 K after each increment. Its shift in field is proportional to the difference between pinned AF entities oriented positively and negatively. A gradual change in the amplitude and sign of H_E is observed (see Fig. 1) since the higher the T_a the more the reversed entities. At each increment of T_a, H_E reflects the difference between AF entities with T_B larger and lower than T_a. It follows by definition that the variations of the derivative $\delta H_E/\delta T_a$ with T_a represent DT_B. Thus (i) an inflection point for H_E vs T_a denotes a peak in the distribution, and (ii) the amplitude of H_E (ΔH_E) around the inflection is the surface of the peak. In the following, ΔH_E is the difference between H_E after Ta = 4 and 200 K (i.e., after the inflection, on the plateau).

[a)]Author to whom correspondence should be addressed. Electronic mail: vincent.baltz@cea.fr

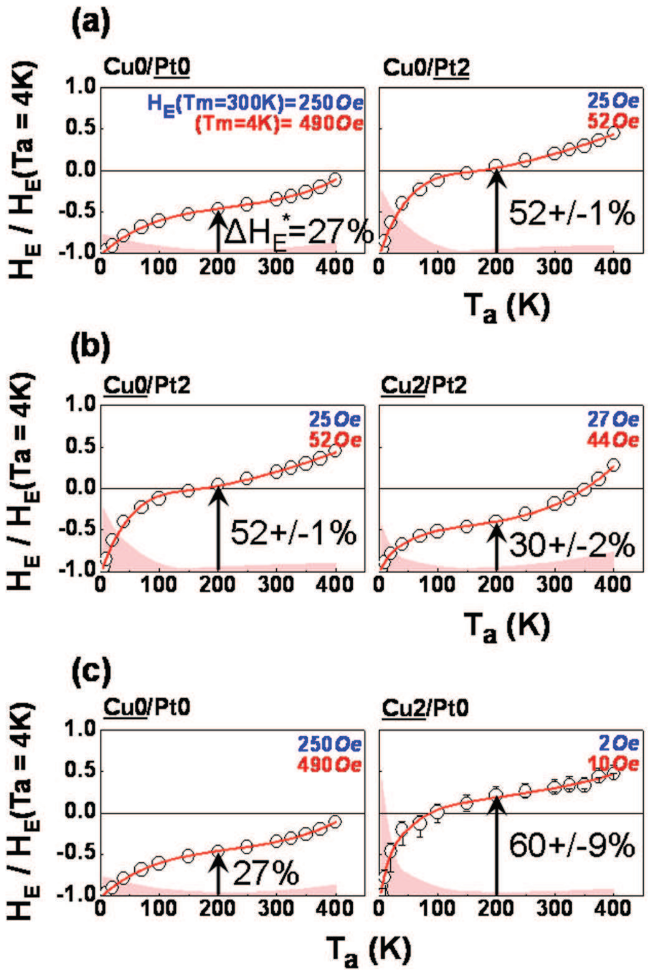

FIG. 1. Front: variations with the annealing temperatures (T_a) of the normalized loop shift ($H_E/|H_E$ ($T_a = 4$ K)|) deduced from hysteresis loops measured at 4 K by VSM along the field cooling (FC) direction for samples with composition: Si/SiO_2//Ta (3 nm)/Cu (3 nm)/Co (3 nm)/Cu (t_{Cu})/Pt (t_{Pt})/IrMn (7 nm)/Pt (2 nm) and subject to a procedure detailed within the text and involving various T_a. The Cu and Pt thicknesses of the Cu/Pt intermixing dual barrier are t_{Cu} and t_{Pt}, respectively: (a) $t_{Cu} = 0$ and varying t_{Pt}; (b) $t_{Pt} = 2$ nm and varying t_{Cu}; and (c) $t_{Pt} = 0$ and varying t_{Cu}. To ease the reading, the plots in Fig. 1(a) for Cu0/Pt0 and Cu0/Pt2 are reproduced in Figs. 1(b) and 1(c), respectively. The full lines in the graphs result from interpolation of the data. Back: variations with T_a of the normalized derivatives $\delta H_E/\delta T_a$ deduced from the full lines. $\delta H_E/\delta T_a$ *vs* T_a represent the blocking temperature distributions. The absolute values of H_E measured at $T_m = 300$ and 4 K after positive FC from 573 K to T_m are indicated.

Figure 1 shows the variations with T_a of the normalized loop shifts, $H_E/|H_E$ ($T_a = 4$ K)| (front) and the corresponding DT_B (back) for Si/SiO_2//Ta (3 nm)/Cu (3 nm)/Co (3 nm)/Cu (t_{Cu})/Pt (t_{Pt})/IrMn (7 nm)/Pt (2 nm) with various intermixing barriers. For all the samples, the low-T contribution to DT_B known to originate from AF interfacial spin-glass-like phases[9–13] is fully observed. Given that ΔH_E also denotes the glassy character of the surface. This is represented by ΔH_E* and arrows in Figs. 1 and 2 and expressed in percentage: ΔH_E* equals ΔH_E normalized to the total expected variations of H_E, i.e., 2 for normalized H_E: from -1 to 1. The beginning of the second inflection point in the H_E vs T_a variations witnesses the high-T contribution to DT_B related to the grains sizes dispersion.[9–13] This contribution exists for all the samples since H_E is due to reach back its maximum amplitude but with opposite sign for larger T_a, i.e., when all the AF entities are reoriented.[12]

It is known that Co-Mn intermixing exists at Co/IrMn interfaces,[4,6,7] and it has been observed that a Pt insertion limits such intermixing,[6,7] which should be beneficial for the interfacial quality. However, Pt is not an inert barrier here since it is fully miscible with Co. As a result, CoPt alloys with reduced ordering T around the Co-Pt interface form.[4,6,7,14] As a consequence, Fig. 1(a) shows that compared to no Pt inclusion, ΔH_E* and thus DT_B increases when a 2 nm thick Pt is inserted (from ∼27 to ∼52%). This confirms that the interfacial quality actually worsened. Figure 1(a) also shows that the thicker the Pt (0; 2, and 4 nm), the larger the ΔH_E* and thus the larger the DT_B contribution (∼21; ∼52 and ∼65%, respectively). This implies that the thicker the Pt insertion, the more glassy the interface. It may mean that the Co or Pt diffusion lengths in our experimental conditions are larger than t_{Pt} or t_{Co}. Pt and Co diffusions through grain boundaries are also not excluded.[6,18] To avoid Co-Pt intermixing in the case of a single Pt barrier we further added a Cu layer, immiscible with Co (Refs. 4 and 26) and obtained a dual (Cu/Pt) barrier. By looking at the plots for (Cu0/Pt2) and (Cu2/P2), Fig. 1(b) shows that this further Cu insertion indeed reduces DT_B (from ∼52 to ∼30%) and therefore increases the interfacial quality. Additionally, Fig. 1(b) shows that for (Cu/Pt2) dual barriers, the thicker the Cu (0; 2 and 4 nm), the smaller the DT_B (∼52; ∼30 and ∼21%, respectively). For similar reasons as above, diffusion length vs film thickness or Co and Pt diffusions via grain boundaries may be argued. It is noticeable that DT_B for a Co/(Cu4/Pt2)/IrMn stack [∼21%, see third plot in Fig. 1(b)], i.e., with an intermixing dual barrier, is smaller than DT_B for a Co/IrMn bilayer [∼27%, see first plot in Fig. 1(b)], i.e., without any intermixing barrier. This thus proves that an efficient inert intermixing barrier is a viable solution to limit the dispersions of T_B in exchange biased stacks, but, as a counterpart, it weakens H_E by taking the F away from the AF (see values in Fig. 1).[25] However, in Fig. 1(b), when comparing (Cu0/Pt2) and (Cu2/P2) we remark that the relative changes of H_E are very limited (from 52 to 44 Oe for a measurement T of 4 K)

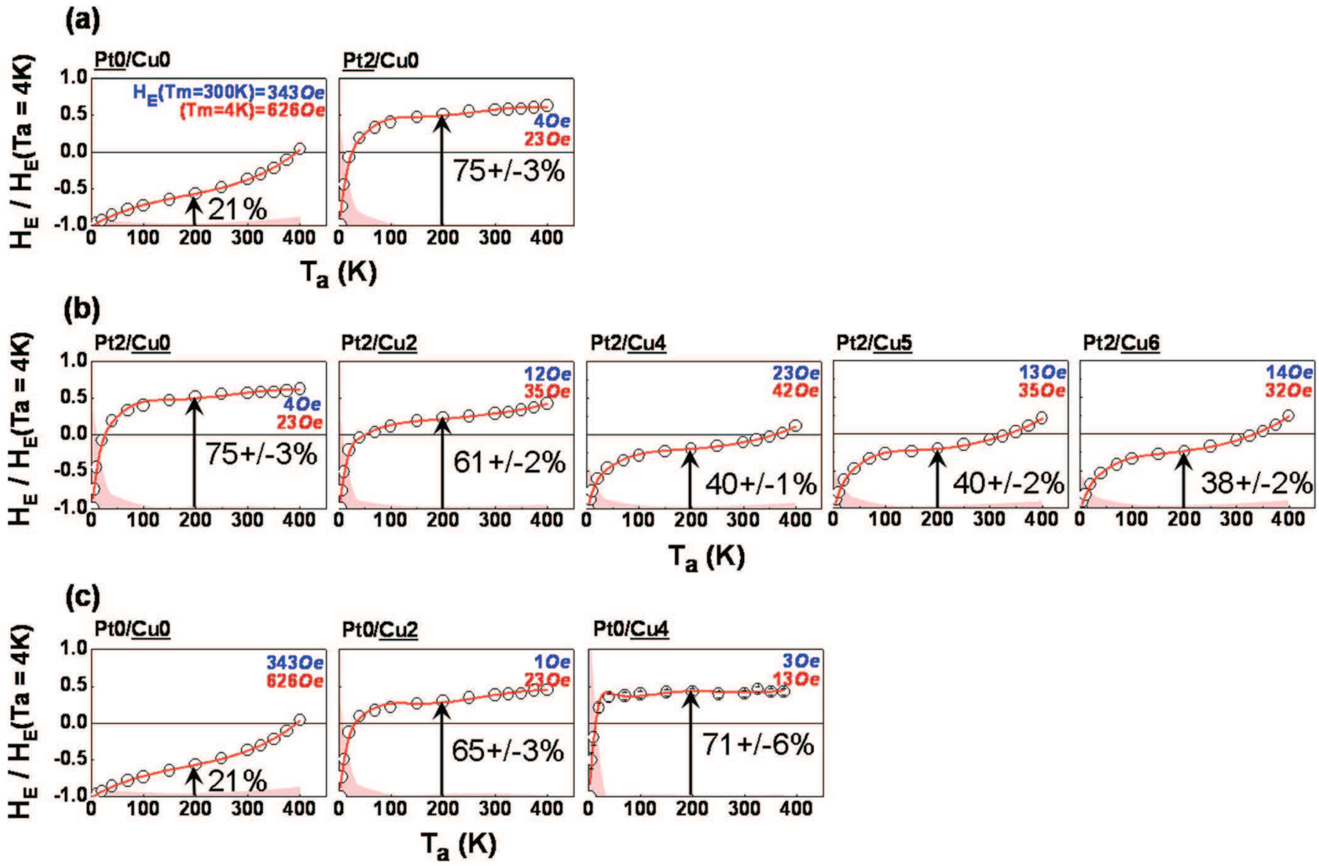

FIG. 2. Front: variations with T_a of $H_E/|H_E\ (T_a = 4\,K)|$ for the inverted structures: Si/SiO_2//Ta (3 nm)/Cu (3 nm)/IrMn (7 nm)/Pt (t_{Pt})/Cu (t_{Cu})/Co (3 nm)/Pt (2 nm) with: (a) $t_{Cu} = 0$ and varying t_{Pt}; (b) $t_{Pt} = 2$ nm and varying t_{Cu}; and (c) $t_{Pt} = 0$ and varying t_{Cu}. The full lines in the graphs result from interpolation of the data. Back: variations with T_a of the normalized derivatives $\delta H_E/\delta T_a$ deduced from the full lines. The absolute values of H_E measured at $T_m = 300$ and 4 K after positive FC from 573 K to T_m are indicated.

despite the addition of as much as 2 nm more between the F and the AF. This result is encouraging and introduces the fact that the benefits of intermixing limitations may, in some conditions, overcome the disadvantages of spacing augment between the F and the AF. Finally, notice that the sole insertion of a single Cu barrier as opposed to a dual (Cu/Pt) barrier leads to larger DT_B; thus, to more glassy interfaces, as concluded from Fig. 1(c), the case (Cu4/Pt0) virtually gave zero loop shift, and no DT_B could be measured. We argue that Cu and Mn are indeed miscible and that CuMn alloys are known to lead to spin-glass phases.[11,17,23,24]

In order to strengthen our findings and confirm that the effect is predominantly driven by layers intermixing and not by potential structural or roughness changes, we systematically performed measurements for the reversed structures. Figure 2 shows the results for Si/SiO_2//Ta (3 nm)/Cu (3 nm)/IrMn (7 nm)/Pt (t_{Pt})/Cu (t_{Cu})/Co (3 nm)/Pt (2 nm). We note that the top and bottom IrMn stacks are certainly not symmetrical due to growth issues on various buffers which influences interface roughness, alloying, layers structures, etc. and affect the H_E absolute values differences between top and bottom stacks.[26,27] For example, although (Cu0/Pt4) and (Pt0/Cu4) based samples gave a non-zero H_E, thus allowing DT_B measurements, the cases (Cu4/Pt0) and (Pt4/Cu0) gave zero H_E, and thus no DT_B could be measured. The origins of the differences between top and bottom IrMn structures were already studied in the literature and are out of the scope of the present paper. Although the absolute values of H_E and ΔH_E* vary between top and bottom IrMn, in agreement with previous results,[27] similar trends were obtained after the addition of the barriers, thus leading to analogous conclusions. This indeed confirms that our relative observations are predominantly related to intermixing. The barriers addition certainly has other consequences, e.g., on roughness, which surely depend on the top or bottom character of the stack, but such other consequences mainly influence the absolute values differences between top and bottom and not the relative trends for a given top or bottom stack. In brief, Fig. 2(a) shows the effect of Pt-Co intermixing when adding a single Pt barrier to limit Mn-Co intermixing, which leads to more glassy interfaces and thus to larger DT_B (~21 and ~75% for $t_{Pt} = 0$ and 2 nm, respectively). Figure 2(c) shows the effect of Cu-Mn intermixing when adding a single Cu barrier, which also leads to larger DT_B (~21; ~65 and ~71% for $t_{Cu} = 0$; 2 and 4 nm, respectively). Finally, Fig. 2(b) confirms the beneficial effect of (Pt/Cu) dual barriers for the reductions of DT_B. The corresponding values of H_E and ΔH_E* are plotted together in Fig. 3(a). When the Cu thickness of the (Pt2/Cu) tandem increases, the interfacial quality improves up to a threshold value ($t_{Cu} = 4$ nm) and levels out above. For our sputtering deposition process (which certainly participate to the activation of some lattice defects within grains[6,7]) and post-deposition annealing (at 573 K for 1 h), diffusion may occur via the core of each grain and via grain boundaries.[18] This may happen up

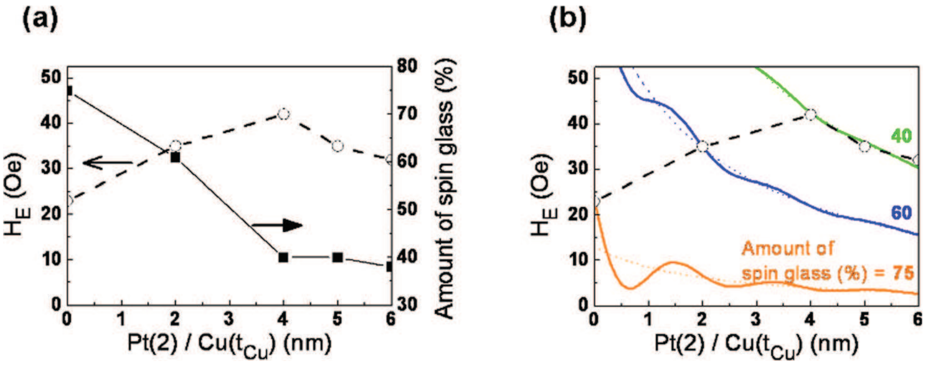

FIG. 3. (a) Variations of the hysteresis loop shift (H_E) measured at 4 K and of the relative amount of spin glass deduced from Fig. 2(b) as a function of the Cu thickness (t_{Cu}) for samples of Si/SiO_2//Ta (3 nm)/Cu (3 nm)/IrMn (7 nm)/Pt (2 nm)/Cu (t_{Cu})/Co (3 nm)/Pt (2 nm). (b) Comparison of the experimental H_E vs t_{Cu} plot reproduced from Fig. 3(a) (data points and dashed line) with series of expected H_E vs t_{Cu} trends for various relative amount of spin glass, i.e., for various interfacial qualities (dotted full lines in color).

to a threshold thickness larger than the diffusion lengths in the grains and grain boundaries. Actually, it is known that, in some conditions, grain boundaries and defects offer paths with enhance atomic mobility, thereby possibly dominating the atomic transport.[18] We also note that our (Pt/Cu) dual barrier is surely a more complex barrier since Pt and Cu do mix.[4] Attempts with (Ru2/Cu2) barriers in which Ru and Cu are not miscible[4] did not show any H_E probably due to Ru and Mn intermixing and to wetting issues of Cu on Ru. This, thus, points out the importance of the choice of the materials in the dual barrier even if these latter are miscible between them and provided that they are efficient barriers for the surrounding materials. From Fig. 3(a), we also observe that H_E first increases when the amount of spin-glass decreases (i.e., when the interfacial quality improves) and then reduces when the amount of spin-glass levels out. Figure 3(b) helps us to explain this behaviour. First note that the exchange interactions between Co and IrMn through 2 nm of Pt plus 2 to 6 nm of Cu (or more likely through a PtCu alloy) are surely mediated by itinerant *s* electrons.[28,29] To a first approximation this sounds plausible, since the spin diffusion lengths in Pt, Cu, and some PtCu alloys can be larger, at 4 K, than the above mentioned characteristic lengths.[30] In particular, an oscillating behaviour of the magnetic properties for [PtCu-alloys/Co] multilayers[28] was already reported in the literature. Additionally, long range interactions have been modelled and experimentally reported in the literature between a F and an AF, although the spacer did not involve Pt nor a Pt based alloys.[31–35] Finally, we attempted (Pt1/AlOx2/Cu1) trilayer barrier. The total barrier thickness was set to 4 nm so as to compare with the (Pt2/Cu2) dual barrier. No loop shift was obtained (hence no distribution could be measured). Since our AlOx is insulating it may break the IrMn-Co long range interaction. This result probably supports the idea of long range mediation via itinerant *s* electrons. In Fig. 3(b), we plotted a series of oscillatory decreasing loops of the form: $A \times \exp(-t/L)/t + B \times (C \times t \times \cos(C \times t) - \sin(C \times t))/(C \times t)$.[4] The first term represents the reduction of H_E ascribed to spacing augment between the F and the AF[25] and the second term models additional RKKY long range interactions.[28] These curves are guides to the eye, and A, B, C, and L have been assigned arbitrary values. B, C, and L were kept constant, while A was increased to model an interfacial improvement. The variable t is the total thickness of the dual barrier. This series of virtual master curves reads as follows: the interface gradually improves when switching from the orange curve (75%) to the dark blue (60%) and to the green curve (40%). The interfacial improvement experimentally measured between 0 and 4 nm of Cu [see Fig. 3(a)] means that the corresponding virtual H_E should jump from master curve to master curve. As shown in Fig. 3(b) this is in agreement with the experimental increase of H_E. When the interfacial quality levels out, above $t_{Cu} = 4$ nm as experimentally observed in Fig. 3(a), the related virtual H_E should stick to the same curve: here, the green curve (40%) in Fig. 3(b). It then follows the decrease due to the gradual separation of the F and the AF, which is also in agreement with the experimental trend. Although adding a diffusion barrier to bare Co/IrMn did not fulfil at once interfacial improvement (i.e., spin-glass reductions) and preservation of a decent value for H_E, for the (Pt2/Cu) series [Fig. 3(a)] we evidenced that, in some conditions and despite the F-AF spacing augment, it was possible, via the addition of diffusion barriers, to simultaneously increase H_E and lower the T_B dispersions.

To conclude, the report of layers intermixing at ferromagnetic/antiferromagnetic exchange biased interfaces and concomitant formation of interfacial spin-glass-like phases with reduced properties and increased dispersions led us to engineer diffusion barriers. Cu and Pt based barriers were inserted at Co/IrMn interfaces, and the interfacial quality potential improvement was investigated via measurements of the low-temperature contributions to the blocking temperature distributions: the smaller the contribution, the less glassy the interface. The use of (Cu/Pt) intermixing dual barriers led to blocking temperature distributions reductions as a result of interfaces improvements. All at once, (Cu/Pt) limited Co-Mn, Co-Pt, and Cu-Mn mixing, which took place when using either no or single Pt and Cu barriers. Although inserting (Cu/Pt) intermixing dual barriers was beneficial for the exchange bias properties dispersions, it weakened the loop shift amplitudes by taking the ferromagnet away from the antiferromagnet. However, some encouraging data suggested that it is in principle possible to find barriers for which the benefits of intermixing limitations overcome the disadvantages of spacing augment between the ferromagnet and the antiferromagnet. Since Cu and Pt are miscible, complementary studies with Cu_xPt_{1-x} barriers would be interesting, although polycrystalline Cu_xPt_{1-x} alloys may also diffuse throughout grain boundaries. Other complementary studies could involve amorphous layers in order to avoid diffusion via grain boundaries.

This work was partially funded by the European Commission via the ERC advanced grant HYMAGINE (No. 246942).

[1] S. A. Wolf, D. D. Awschalom, R. A. Buhrman, J. M. Daughton, S. von Molna, M. L. Roukes, A. Y. Chtchelkanova, and D. M. Treger, Science **294**, 1488 (2001).
[2] J. Nogués and I. K. Schuller, J. Magn. Magn. Mater. **192**, 203 (1999).
[3] A. E. Berkowitz and K. Takano, J. Magn. Magn. Mater. **200**, 552 (1999).
[4] R. M. Bozorth, *Ferromagnetism* (D. Van Nostrand Company, Inc., 1951).
[5] X. W. Zhou, H. N. G. Wadley, R. A. Johnson, D. J. Larson, N. Tabat, A. Cerezo, A. K. Petford-Long, G. D. W. Smith, P. H. Clifton, R. L. Martens, and T. F. Kelly, Acta Mater. **49**, 4005 (2001).
[6] L. Lechevallier, A. Zarefy, F. Letellier, R. Lardé, D. Blavette, J. M. Le Breton, V. Baltz, B. Rodmacq, and B. Dieny, J. Appl. Phys. **112**, 043904 (2012).
[7] F. Letellier, V. Baltz, L. Lechevallier, R. Lardé, J.-F. Jacquot, B. Rodmacq, J.-M. Le Breton, and B. Dieny, J. Phys. D: Appl. Phys. **45**, 275001 (2012).
[8] A. P. Malozemoff, Phys. Rev. B **35**, 3679 (1987).
[9] K. Takano, R. H. Kodama, A. E. Berkowitz, W. Cao, and G. Thomas, Phys. Rev. Lett. **79**, 1130 (1997).
[10] J. Ventura, J. P. Araujo, J. B. Sousa, A. Veloso, and P. P. Freitas, J. Appl. Phys. **101**, 113901 (2007).
[11] M. Ali, P. Adie, C. H. Marrows, D. Greig, B. J. Hickey, and R. L. Stamps, Nat. Mater. **6**, 70 (2007).
[12] V. Baltz, B. Rodmacq, A. Zarefy, L. Lechevallier, and B. Dieny, Phys. Rev. B **81**, 052404 (2010).
[13] K. O'Grady, L. E. Fernandez-Outon, and G. Vallejo-Fernandez, J. Magn. Magn. Mater. **322**, 883 (2010).
[14] V. Baltz and B. Dieny, J. Appl. Phys. **109**, 066102 (2011).
[15] V. Baltz, Appl. Phys. Lett. **102**, 062410 (2013).
[16] L. E. Fernandez-Outon, M. S. Araújo Filho, R. E. Araújo, J. D. Ardisson, and W. A. A. Macedo, J. Appl. Phys. **113**, 17D704 (2013).
[17] D. Kaya, P. N. Lapa, P. Jayathilaka, H. Kirby, C. W. Miller, and I. V. Roshchin, J. Appl. Phys. **113**, 17D717 (2013).
[18] M.-A. Nicolet, Thin Solid Films **52**, 415 (1978).
[19] S. Song, Y. Liu, M. Li, D. Mao, C. Chang, and H. Ling, Microelectron. Eng. **83**, 423 (2006).
[20] M.-G. Sung, Y. S. Kim, S. J. Kim, I.-K. Jeong, H.-S. Choi, M.-S. Kim, H. Kim, and S.-K. Park, Solid-State Electron. **69**, 22 (2012).
[21] S. Soeya, T. Imagawa, S. Mitsuoka, and S. Narishige, J. Appl. Phys. **76**, 5356 (1994).
[22] E. Fulcomer and S. H. Charap, J. Appl. Phys. **43**, 4190 (1972).
[23] P. Gibbs, T. M. Harden, and J. H. Smith, J. Phys. F: Met. Phys. **15**, 213 (1985).
[24] R. K. Chouhan and A. Mookerjee, J. Magn. Magn. Mater. **323**, 868 (2011).
[25] N. J. Gökemeijer, T. Ambrose, and C. L. Chien, Phys. Rev. Lett. **79**, 4270 (1997).
[26] S. Bandiera, R. C. Sousa, B. Rodmacq, and B. Dieny, Appl. Phys. Lett. **100**, 142410 (2012).
[27] V. Baltz, S. Auffret, and B. Dieny, IEEE Trans. Mag. **47**, 3308 (2011).
[28] Y. J. Wang, Appl. Phys. A **68**, 231 (1999).
[29] P. Bruno and C. Chappert, Phys. Rev. B **46**, 261 (1992).
[30] J. Bass and W. P. Pratt, Jr., J. Phys.: Condens. Matter **19**, 183201 (2007).
[31] Y.-J. Lee, C.-R. Changa, T.-M. Hong, C. H. Hoa, and M.-T. Lin, J. Magn. Magn. Mater. **240**, 264 (2002).
[32] J. W. Cai, W. Y. Lai, J. Teng, F. Shen, Z. Zhang, and L. M. Mei, Phys. Rev. B **70**, 214428 (2004).
[33] Y.-Y. Song, D.-H. Kim, S.-C. Yu, P. D. Kim, I. A. Turpanov, L. A. Lee, A. E. Buzmakov, and K. W. Lee, J. Appl. Phys. **103**, 07C112 (2008).
[34] A. Paul, N. Paul, J. Jutimoosik, R. Yimnirun, S. Rujirawat, B. Höpfner, I. Lauermann, M. Lux-Steiner, S. Mattauch, and P. Böni, Phys. Rev. B **87**, 014431 (2013).
[35] A. Tan, J. Li, C. A. Jenkins, E. Arenholz, A. Scholl, C. Hwang, and Z. Q. Qiu, Phys. Rev. B **86**, 064406 (2012); Y. Meng, J. Li, P.-A. Glans, C. A. Jenkins, E. Arenholz, A. Tan, J. Gibbons, J. S. Park, C. Hwang, H. W. Zhao, and Z. Q. Qiu, *ibid.* **85**, 014425 (2012).